THE UNIVERSITY OF ADELAIDE
AUSTRALIA

Investigation of External Acoustic Loadings on a Launch Vehicle Fairing During Lift-off

Mir Md. Maruf Morshed

Supervisors:

Professor Colin H. Hansen

Associate Professor Anthony C. Zander

School of Mechanical Engineering

University of Adelaide

South Australia 5005

AUSTRALIA

Dissertation Submitted for the Award of the Degree of Doctor of Philosophy on the 19th May, 2008. Qualified on the 26th August, 2008.

This page intentionally contains only this sentence.

Abstract

During the lift-off of a launch vehicle, the acoustic pressure fluctuations caused by the engine exhaust gases produce high noise levels inside the cavity of the fairing and can damage the payload inside the fairing. Hence reducing the noise transmitted into the payload bay is an important area of research. Work presented in this thesis investigates the external acoustic pressure excitations on the fairing of a launch vehicle during the lift-off acoustic environment. In particular, it investigates the external sound pressure levels in the low frequency range from 50Hz to 400Hz, on the fairing during the lift-off of a launch vehicle.

This study establishes theoretical and numerical models for the prediction of external sound pressure loading on composite structures representing launch vehicles, such as a large composite cylinder referred to as a Boeing cylinder and a Representative Small Launch Vehicle Fairing (RSLVF). To predict the external sound pressure loading, various incident wave conditions were investigated, including incident plane waves, oblique plane waves and oblique plane waves with random phases that strike the circumference of the composite structures.

For the theoretical model, both the incident and scattered sound pressure fields due to incident plane waves; perpendicular to an idealised long cylinder were investigated. The results show that the scattered sound pressure field plays a major role in determining the total circumferential sound pressure field at the surface of the cylinder and cannot be ignored for the launch case.

The theoretical model was developed further for a point source, line source and oblique incident waves, and modified to determine the incident, scattered and total sound pressure fields away from the cylinder. The approach developed overcomes some limitations of previous analytical derivations.

An experiment was undertaken to determine the sound pressure patterns at the surface of a cylinder at various frequencies due to a point source positioned at a finite distance from the cylinder surface. The experimental work confirmed the accuracy of the theoretical model for a point source at a finite distance from the cylinder.

The Boundary Element Method (BEM), approach was used for the numerical investigation of the acoustic loadings. The numerical analysis was developed for various acoustic loading conditions and verified with the theoretical results, which showed that the numerical and theoretical models agree well. Both models were extended to a Boeing composite cylinder and an RSLVF for various acoustic loading conditions.

The complex acoustic environment generated during the lift-off of a launch vehicle was investigated and used as a basis for the acoustic loading on an RSLVF. To predict the acoustic excitations on an RSLVF, two different source allocation techniques were investigated, which considered acoustic sources along the rocket engine exhaust flow. The investigations were conducted both numerically and analytically. Both results agree well and show that it is possible to predict the acoustic loads on the fairing numerically and analytically.

Statement of Originality

To the best of my knowledge and belief, all the material presented in this thesis, except where otherwise referenced, is my own original work, and has not been published previously for the award of any other degree or diploma in any university. If accepted for the award of the degree of Doctor of Philosophy, I consent that this thesis be made available for loan and photocopying.

Mir Md. Maruf Morshed

Date:

Acknowledgement

I would like to acknowledge the efforts of all the people who have made a contribution toward this thesis. Many thanks to my parents, Mir Md. Morshed Ali and Shahana Morshed, who encouraged my mathematical and scientific interests from an early age, made many sacrifices to ensure I received a good education and to their financial support for this study. I would also like to thank my brother Mir Md. Mahmud Morshed and his wife Amy Louise Morshed, for their valuable support while finishing.

I am especially grateful to Professor Colin H. Hansen and Associate Professor Anthony C. Zander, for their supervision and support throughout the entire research. Without their direction and guidance, this thesis would most likely never have been completed. Thanks also to Karen Adams for her contribution to the writing corrections made to this thesis. I would also like to thank Dr Rick Morgans, Dr Carl Q. Howard and Dr Xun Li, for all of their discussions and advice. I am indebted to Silvio De Ieso, Norio Itsumi, Philip Schmidt, Joel Walker and Richard Pateman, for all their help with the design and construction of the electronics and experimental apparatus.

Finally, I would like to express my gratitude to Patricia Anderson, International Student Centre Manager, who handled my visa status during the stay in Australia.

This dissertation is dedicated to all of my family members, especially to my sister Maisha Tasnim and to brother's son who is my little nephew Mir Md. Zebediah Morshed.

Contents

List of Tables

List of Figures

Glossary of Symbols

$\boldsymbol{a}$	Radius of a cylinder
a	Observation point
$\boldsymbol{a_e}$	Speed of sound in the exhaust flow
A_m	Coefficients [defined by equations (3.16)]
b	Distance between two point sources [see Figure (5.8)]; also, frequency band (Ch.9)
c	Speed of sound
$C(q)$	Solid angle from volume V [defined by equations (8.7)]
d	Distance between the nearest source and the cylinder surface [see Figure (5.8)]
D_e	Nozzle exit diameter
E_m^i	Amplitudes of the incident waves [see equation (3.22)]
E_m^o	Amplitudes of the outgoing waves [see equations (3.22), (3.26) and (3.27)]
f	Frequency of sound
F	Driving force in the medium (Ch.3); also, thrust of the rocket engine (Ch.9)
$G(a/r'), G(r_p, r_q),$ $G(R)$	Acoustic Green's function [see equations (5.1), (5.2) and (8.1)]
H_m	Bessel function of the 3rd kind or Hankel function
H_{m+1}	Hankel Function of $(m+1)$th order
H_{m-1}	Hankel Function of $(m-1)$th order
$H_m^1(z)$	Hankel function for incoming waves [defined by equation (A.5)]
$H_m^2(z)$	Hankel function for outgoing waves [defined by equation (A.6)]
H_m'	Derivatives of the Hankel function of mth order
H_0'	Derivatives of the Hankel function of 0th order
H_1	Derivatives of the Hankel function of first order
$I^s(r,k,\phi_i)$	Scattered sound intensity as a function of radial distance r, wavelength k and azimuthal angle ϕ_i [defined by equation (4.4)]
J_m	Bessel function of the first kind of mth order
J_m'	Derivatives of the mth order Bessel function
J_{m+1}	Bessel function of $(m+1)$th order
J_{m-1}	Bessel function of $(m-1)$th order
J_0'	Derivatives of the 0th order Bessel function
J_1	Bessel function of first order

k	Wave number
L	Length of a cylinder
L_{p,b,ϕ_i}	Sound pressure level at a frequency band b of interest [defined by equation (9.8)]
L_{p,OA,ϕ_i}	Overall sound pressure level [defined by equation (9.9)]
L_{p,seg,b,ϕ_i}	Sound pressure level corresponding to each segment at a frequency band b of interest [defined by equation (9.14)]
$L_{p,\mathrm{OA},seg,b,\phi_i}$	Overall sound pressure level over the entire segments of the exhaust flow at a frequency band b of interest [defined by equation (9.15)]
L_w	Overall acoustic power level [defined by equation (9.2)]
$L_{w,b}$	Acoustic power level at a frequency band b of interest [defined by equation (9.5)]
$L_{w,seg}$	Overall acoustic power level of exhaust flow segments [defined by equation (9.10)]
$L_{w,seg,b}$	Acoustic power level of exhaust flow segments at a frequency band b of interest [defined by equation (9.11)]
n	Number of the point sources (Chs.5, 7); also, number of nozzles (Ch.9)
N	Total number of point sources (Ch.5); also, number of surface elements (Ch.8)
$N_i(\xi)$	Element shape functions [see equation (8.11)]
N_m	Bessel function of the 2nd kind or Neumann function
N'_m	Derivatives of the mth order Neumann function
N_{m+1}	Neumann function of the $(m+1)$th order
N_{m-1}	Neumann function of the $(m-1)$th order
N'_0	Derivatives of the 0th order Neumann function
N_1	Neumann function of first order
$p(a,\phi_i)$	Resultant pressure as a function of cylinder radius a and azimuthal angle ϕ_i [defined by equations (3.21) and (3.24)]
p_a	Resultant sound pressure at the surface of a cylinder [defined by equation (3.26)]
p^i	Incident wave pressure [see equation (3.7)]
P	Acoustic pressure
$P(p), P(r_p)$	Acoustic pressure at a point p (Ch.8)
$P(p),\ P_i(p)$	Constant nodal pressure on a point p ; also, constant nodal pressure for ith elements [see equations (8.9) and (8.10)]
P_o	Equilibrium pressure in the medium
$P_{s\infty}(r,\phi)$	Scattered sound pressure as a function of radial distance r and azimuthal angle ϕ [defined by equation (3.20)]
P^i	Incident wave pressure [defined by equation (7.1)]
$P^i(a,k,\phi_i)$	Incident wave pressure as a function of cylinder radius a , wave number k and azimuthal angle ϕ_i [defined by equation (3.10)]

$P^i(r,k,\phi_i)$	Incident sound pressure as a function of radial distance r, wave number k and azimuthal angle ϕ_i [defined by equation (4.1)]
P^s, p_s	Scattered sound pressure
$P^s(a,k,\phi_i)$	Scattered sound pressure as a function of cylinder radius a, wave number k and azimuthal angle ϕ_i [defined by equation (3.11)]
$P^s(r,k,\phi_i)$	Scattered pressure as a function of radial distance r, wave number k and azimuthal angle ϕ_i [defined by equation (4.3)]
$P^I(q)$	Incident acoustic pressure at point q (Ch.8)
P_f^I	Incident acoustic pressure on the field points [see equation (8.18)]
$P_a^t(a,k,\phi_i)$	Total sound pressure as a function of cylinder radius a, wave number k and azimuthal angle ϕ_i [defined by equation (3.18)]
$P_a^t(R_i,k,a,\phi_i,Q_s)$	Total sound pressure at the surface of a cylinder due to a point source [defined by equation (5.5)]
$P'(R_i)$	Spatially dependent factor [defined by equation (5.4)]
Q_s, $Q_{s,b}$, $Q_{s,seg,b}$	Source strength [see equations (5.4), (9.7) and (9.13)]
r_n	Distance between the origin of the cylinder to the nth number of point sources [defined by equation (5.6)]
r_p	Distance to integration point on the boundary from the centre of the body (Ch.8)
r_q	Distance to point q from the centre of the body (Ch.8)
r'	Source distance [see equation (5.1)]
R	Distance between a point source and observation point [see equation (5.2)]; also, oblique resultant distance between a point source and an observation point [defined by equation (7.3)]
R_i	Distances between a point source and ith number of observation points [see equations (5.3) and (7.4)]
R'	Distance between a point source and an projected observation point [see Figure (7.1); also, defined by equation (7.2)]
S	Boundary surface (Ch.8)
t	Time
$\boldsymbol{u}$	Directional particle velocity
$u(p), u_n(r_p)$	Outward normal particle velocity at a point p (Ch.8)
U_e	Fully expanded exit velocity
W_b	Acoustic power of a source at a frequency band b of interest [defined by equation (9.6)]
$W_{seg,b}$	Acoustic power of a source corresponding to a segment of exhaust flow at a frequency band b of interest [defined by equation (9.12)]
x	Distance travelled by sound waves along the x-axis; also, node position along the x coordinate (Ch.8)

x_t	Core length
y	node position along the y coordinate (Ch.8)
z	Cylinder axis
ω	Angular frequency
β	Elevation angle
γ	Specific heat ratio
γ_m	Phase angles for *m*th order
ϕ_i	Azimuthal or circumferential angle
ψ , ψ_s	Velocity potential
$\psi_m^s(a,k,\phi_i)$	Velocity potential as a function of cylinder radius a , wavelength k and azimuthal angle ϕ_i [defined by equation (4.2)]
λ	Wavelength
ρ	Density of air in the exhaust flow
ρ_o	Equilibrium density in the fluid
$\delta(a-r'),\ \delta(r_p-r_q)$	Dirac delta function [see equations (5.1) and (8.1)]
Γ	Gamma function [defined by equation (A.3)]
ε_m	Constant terms used in the equations
∇	Laplacian operator or differential operator
Δx	Length of exhaust flow slices
Δf_b	Bandwidth of the frequency band, b

Appendix A

A. *Bessel's* Differential Equation

The *Bessel functions*, *Neumann functions* and *Hankel functions* are also known as cylindrical functions or *Bessel functions of the first*, *second* and *third kind* respectively, and are the solutions of well known *Bessel's differential equation* (McLachlan, 1941)

$$z^2\left(\frac{d^2y}{dz^2}\right)+z\left(\frac{dy}{dz}\right)+\left(z^2-m^2\right)y=0, \tag{A.1}$$

where $z = ka$. To understand the derivations of the above differential equation in terms of different types of *Bessel functions* the reader can consult with Kreyszig (1983), Morse & Ingard (1986) and Abramowitz & Stegun (1965).

A.1 *Bessel Function of the First Kind* (J_m)

The first linear independent solutions of the above second order differential equation are given by (Abramowitz & Stegun, 1965)

$$J_m(z)=\left(\frac{z}{2}\right)^m\sum_{k=0}^{\infty}\frac{\left(-\frac{z2}{4}\right)^k}{k!\Gamma(m+k+1)}, \tag{A.2}$$

which is the *Bessel function of the first kind* of order m. $\Gamma(m)$ is the *gamma function* and defined by the integral (Kreyszig, 1983)

$$\Gamma(m)=\int_0^{\infty}e^{-t}\,t^{m-1}\,dt \tag{A.3}$$

Figure A1 shows the variations in amplitudes of different orders of the *Bessel functions of*

the first kind with respect to the argument z, where J_0 is finite and $J_1 = 0$; when $z = 0$. For each case, the amplitude of J_m decreases and tends to zero as the value of argument z increases. The values of J_m calculated using MATLAB are also provided in Tables A1 to A8. The values of J_m corresponding to the values of m = 0, 1 and 2 have been verified with Abramowitz & Stegun (1965, Table 9.1).

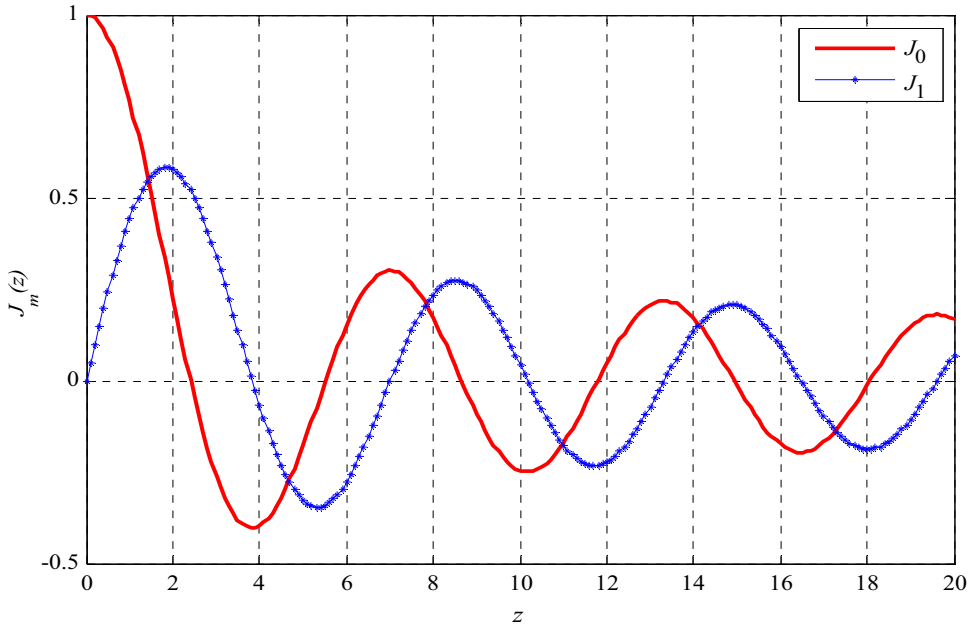

Figure A1: Characteristic behavior of *Bessel functions of the first kind* of order 0, and 1 with respect to the argument z.

A.2 *Bessel Function of the Second Kind* (N_m)

Also known as *Neumann function* and denoted by N_m. The *Neumann function* is the second linear independent solution of the second order differential equation (A.1) and defined as (Abramowitz & Stegun, 1965; Kreyszig, 1983)

$$N_m = \frac{\left[J_m(z)\cos m\pi - J_{-m}(z)\right]}{\sin m\pi}. \qquad \text{A.4}$$

Figure A2 shows the variations in amplitudes of the *Bessel functions of the second kind* of order zero and one with respect to the argument z, where N_0 and N_1 are infinite when $z = 0$. For each case, the amplitude of N_m decreases and tends to zero as the value of the argument z increases. The values of N_m calculated using MATLAB are also provided in Tables A1 to A8. The values of N_m corresponding to the values of m = 0, 1 and 2 have been verified with Abramowitz & Stegun (1965, Table 9.1).

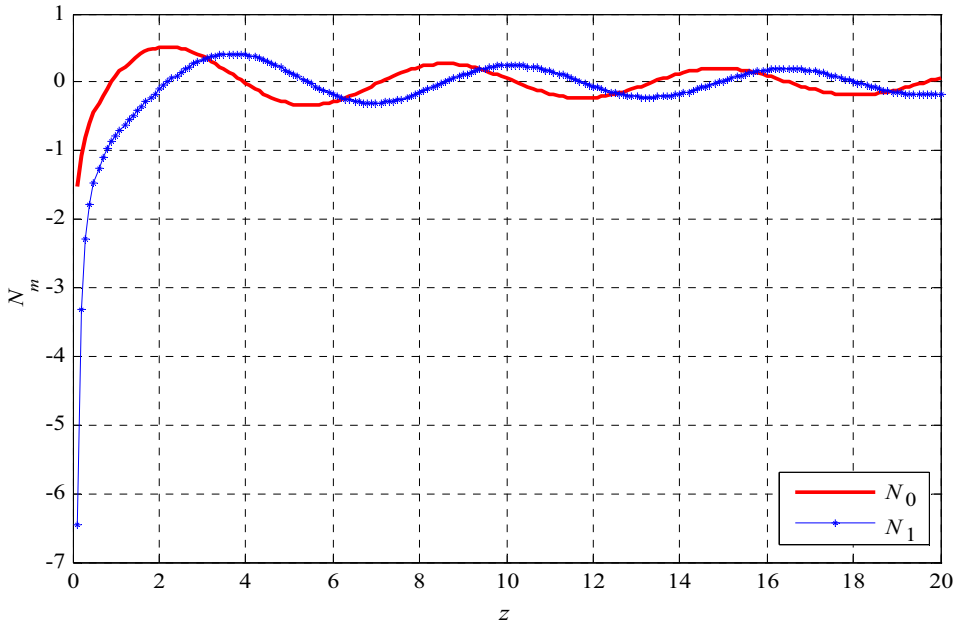

Figure A2: Characteristic behaviour of *Bessel functions of the second kind* of order 0 and 1 with respect to the argument z.

A.3 *Bessel Function of the Third Kind* (H_m)

Also known as *Hankel function* and denoted by H_m. This is the combination of *Bessel function of first* J_m and *second kind* N_m respectively. The relationships between the *Hankel function* and *Bessel functions* are as follows:

$$H_m^{(1)}(z) = J_m(z) + i\,N_m(z), \qquad \text{A.5}$$

$$H_m^{(2)}(z) = J_m(z) - i\,N_m(z), \qquad \text{A.6}$$

where the superscripts (1) and (2) represent the incoming waves and outgoing waves, respectively. The superscript (2) has been used in this thesis for the scattered waves.

Table A.1: Values of cylindrical *Bessel functions* calculated using MATLAB for $ka = 1$.

m	$J_m(ka)$	$N_m(ka)$
0	0.76519768655797	0.08825696421568
1	0.44005058574493	-0.78121282130029
2	0.11490348493190	-1.65068260681625
3	0.01956335398267	-5.82151760596473
4	0.00247663896411	-33.27842302897213
5	2.497577302112346e-004	-2.604058666258123e+002
6	2.093833800238928e-005	-2.570780243229151e+003
7	1.502325817436808e-006	-3.058895705212400e+004
8	9.422344172604498e-008	-4.256746184865068e+005
9	5.249250179911874e-009	-6.780204938731985e+006
10	2.630615123687453e-010	-1.216180142786892e+008
11	1.198006746303138e-011	-2.425580080635053e+009
12	4.999718179448416e-013	-5.324114375969247e+010
13	1.925616764480169e-014	-1.275361870151984e+012
14	6.885408200044238e-016	-3.310616748019190e+013
15	2.297531532210353e-017	-9.256973275752211e+014

Table A.2: Values of cylindrical *Bessel functions* calculated using MATLAB for $ka = 3$.

m	$J_m(ka)$	$N_m(ka)$
0	-0.26005195490193	0.37685001001279
1	0.33905895852594	0.32467442479180
2	0.48609126058589	-0.16040039348492
3	0.30906272225525	-0.53854161610503
4	0.13203418392461	-0.91668283872514
5	0.04302843487705	-1.90594595382867
6	0.01139393233221	-5.43647034070377
7	0.00254729445180	-19.83993540898641
8	4.934417762088341e-004	-87.14989490123281
9	8.439502130909183e-005	-4.449595040642552e+002
10	1.292835164571588e-005	-2.582607129484299e+003
11	1.793989662347444e-006	-1.677242135916440e+004
12	2.275725448320574e-007	-1.204151495043880e+005
13	2.659069630901111e-008	-9.465487746759396e+005
14	2.880156512705533e-009	-8.083007564353754e+006
15	2.907644762406028e-010	-7.449485515929242e+007

Table A.3: Values of cylindrical *Bessel functions* calculated using MATLAB for $ka = 5$.

m	$J_m(ka)$	$N_m(ka)$
0	-0.17759677131434	-0.30851762524903
1	-0.32757913759147	0.14786314339123
2	0.04656511627775	0.36766288260552
3	0.36483123061367	0.14626716269319
4	0.39123236045865	-0.19214228737369
5	0.26114054612017	-0.45369482249110
6	0.13104873178169	-0.71524735760851
7	0.05337641015589	-1.26289883576932
8	0.01840521665480	-2.82086938254560
9	0.00552028313948	-7.76388318837658
10	0.00146780264731	-25.12911009561009
11	3.509274497662084e-004	-92.75255719406377
12	7.627813166084566e-005	-3.829821415582704e+002
13	1.520758220584946e-005	-1.745561722285635e+003
14	2.801295809571661e-006	-8.693938814327028e+003
15	4.796743277517957e-007	-4.694049563794573e+004

Table A.4: Values of cylindrical *Bessel functions* calculated using MATLAB for $ka = 10$.

m	$J_m(ka)$	$N_m(ka)$
0	-0.24593576445135	0.05567116728360
1	0.04347274616886	0.24901542420695
2	0.25463031368512	-0.00586808244221
3	0.05837937930519	-0.25136265718384
4	-0.21960268610201	-0.14494951186809
5	-0.23406152818679	0.13540304768936
6	-0.01445884208479	0.28035255955746
7	0.21671091768505	0.20102002377959
8	0.31785412684386	0.00107547373396
9	0.29185568526512	-0.19929926580524
10	0.20748610663336	-0.35981415218340
11	0.12311652800160	-0.52032903856156
12	0.06337025497016	-0.78490973265203
13	0.02897208392678	-1.36345431980331
14	0.01195716323946	-2.76007149883658
15	0.00450797314372	-6.36474587693912
16	0.00156675619170	-16.33416613198079
17	5.056466697193248e-004	-45.90458574539942
18	1.524424853455242e-004	-1.397414254023773e+002
19	4.314627752456253e-005	-4.571645457031588e+002
20	1.151336924781339e-005	-1.597483848269627e+003

Table A.5: Values of cylindrical *Bessel functions* calculated using MATLAB for $ka = 15$.

m	$J_m(ka)$	$N_m(ka)$
0	-0.01422447282678	0.20546429603892
1	0.20510403861352	0.02107362803687
2	0.04157167797525	-0.20265447896734
3	-0.19401825782012	-0.07511482242816
4	-0.11917898110330	0.17260854999607
5	0.13045613456503	0.16717271575940
6	0.20614973747999	-0.06116007282314
7	0.03446365541896	-0.21610077401791
8	-0.17398365908896	-0.14053398292691
9	-0.22004622511385	0.06619785889587
10	-0.09007181104766	0.21997141360196
11	0.09995047705030	0.22709735924007
12	0.23666584405477	0.11310471328348
13	0.27871487343733	-0.04612981798650
14	0.24643993656993	-0.19306306446008
15	0.18130634149321	-0.31425456900565
16	0.11617274641649	-0.43544607355122
17	0.06652885086197	-0.61469705457029
18	0.03462598220398	-0.95786725014144
19	0.01657350642758	-1.68418434576916
20	0.00736023407922	-3.30873309247376
21	0.00305378445035	-7.13910390082753
22	0.00119036238175	-16.68075782984334
23	4.379452027907171e-004	-41.79111906671292
24	1.526695734729023e-004	-1.114786739747429e+002
25	5.059743232257010e-005	-3.149406376524644e+002
26	1.598853426899810e-005	-9.383234515334716e+002
27	4.829486476623289e-006	-2.937913994330237e+003
28	1.397617046845745e-006	-9.638166928055382e+003
29	3.882838316008275e-007	-3.304457587040985e+004
30	1.037471020107873e-007	-1.181341931041960e+005

Table A.6: Values of cylindrical *Bessel functions* calculated using MATLAB for $ka = 20$.

m	$J_m(ka)$	$N_m(ka)$
0	0.16702466434058	0.06264059680938
1	0.06683312417585	-0.16551161436252
2	-0.16034135192300	-0.07919175824564
3	-0.09890139456045	0.14967326271339
4	0.13067093355486	0.12409373705965
5	0.15116976798239	-0.10003576788953
6	-0.05508604956367	-0.17411162100442
7	-0.18422139772059	-0.00443120471312
8	-0.07386892884075	0.17100977770524
9	0.12512625464799	0.14123902687731
10	0.18648255802395	-0.04389465351566
11	0.06135630337595	-0.18513368039297
12	-0.11899062431040	-0.15975239491661
13	-0.20414505254843	-0.00656919350696
14	-0.14639794400256	0.15121244335756
15	-8.120690551536038e-004	0.21826661420754
16	0.14517984041983	0.17618747795375
17	0.23309981372688	0.06363335051846
18	0.25108984291587	-0.06801078207236
19	0.21886190352168	-0.18605275824872
20	0.16474777377533	-0.28548945860020
21	0.11063364402897	-0.38492615895169
22	0.06758287868551	-0.52285547519834
23	0.03804868907916	-0.76535588648466
24	0.01992910619655	-1.23746306371638
25	0.00978116579257	-2.20455546643466
26	0.00452380828487	-4.27392560237026
27	0.00198073574809	-8.90765109972802
28	8.241782349825159e-004	-19.77673236689541
29	3.269633098572617e-004	-46.46719952757916
30	1.240153636035431e-004	-1.149781462630842e+002
31	4.508278095336757e-005	-2.984672392616736e+002
32	1.574125735189640e-005	-8.102702954481043e+002
33	5.289242572700920e-006	-2.294397706172262e+003
34	1.713243138016636e-006	-6.761242134920362e+003
35	5.357840965556445e-007	-2.069382555255698e+004

Table A.7: Values of cylindrical *Bessel functions* calculated using MATLAB for $ka = 25$.

m	$J_m(ka)$	$N_m(ka)$
0	0.09626678327596	-0.12724943226801
1	-0.12535024958029	-0.09882996478324
2	-0.10629480324238	0.11934303508535
3	0.10834308106151	0.11792485039689
4	0.13229714269714	-0.09104107099009
5	-0.06600799539842	-0.14705799311372
6	-0.15870034085651	0.03221787374460
7	-0.01016816821270	0.16252257251113
8	0.15300616665740	0.05879476686163
9	0.10809211487344	-0.12489392171969
10	-0.07517984394852	-0.14871839049981
11	-0.16823599003226	0.00591920931984
12	-0.07286782727986	0.15392729470127
13	0.09828287584359	0.14185099359337
14	0.17508201815719	-0.00640226136416
15	0.09780898449247	-0.14902152632123
16	-0.05771123676623	-0.17242357022132
17	-0.17167936755325	-0.07168064356206
18	-0.17577270310618	0.07493789497692
19	-0.08143332491966	0.17959121232883
20	0.05199404922830	0.19804074776289
21	0.16462380368494	0.13727398409180
22	0.22457394096240	0.03257954551133
23	0.23062633240888	-0.07993398399185
24	0.19977851066994	-0.17965807605634
25	0.15294840807741	-0.26500952203633
26	0.10611830548487	-0.35036096801631
27	0.06777766733113	-0.46374129143760
28	0.04028145595036	-0.65132022148891
29	0.02245279399769	-0.99521600469755
30	0.01180902612427	-1.65758090940941
31	0.00588886870056	-2.98297817788503
32	0.00279536825312	-5.74020497174547
33	0.00126727402742	-11.71194654978338
34	5.502351792759557e-004	-25.17933391968267
35	2.293656602088348e-004	-56.77584171175352
36	9.198866930878187e-005	-1.337930228732272e+002
37	3.556170740045715e-005	-3.285480641631411e+002
38	1.327398459657133e-005	-8.387092470496709e+002
39	4.791205773119736e-006	-2.221128046867860e+003
40	1.674577415562247e-006	-6.091210259178055e+003

Table A.8: Values of cylindrical *Bessel functions* calculated using MATLAB for $ka = 30$.

m	$J_m(ka)$	$N_m(ka)$
0	-0.08636798358104	-0.11729573168666
1	-0.11875106261662	0.08442557066175
2	0.07845124607327	0.12292410306411
3	0.12921122875972	-0.06803569025320
4	-0.05260900032132	-0.13653124111475
5	-0.14324029551208	0.03162735928926
6	0.00486223515063	0.14707369421118
7	0.14518518957233	0.02720211839521
8	0.06289085331646	-0.13437937229341
9	-0.11164340113688	-0.09887111695169
10	-0.12987689399859	0.07505670212240
11	0.02505880513782	0.14890891836662
12	0.14825335109966	0.03414317134646
13	0.09354387574190	-0.12159438128946
14	-0.06718199212334	-0.13952496846399
15	-0.15624706839036	-0.00862892261027
16	-0.08906507626701	0.13089604585372
17	0.06124432037221	0.14825137152090
18	0.15847530602218	0.03712217520330
19	0.12892604685441	-0.10370476127694
20	0.00483101999340	-0.16848153948743
21	-0.12248468686321	-0.12093729137296
22	-0.17630958160189	-8.306684347197038e-004
23	-0.13610269948624	0.11971897766871
24	-0.03238122427700	0.18439976752674
25	0.08429274064303	0.17532065037407
26	0.17286912534872	0.10780131643005
27	0.21534707662809	0.01153496477135
28	0.21475561258184	-0.08703837984162
29	0.18553006685800	-0.17400660714238
30	0.14393585001031	-0.24937439396697
31	0.10234163316261	-0.32474218079157
32	0.06757019185909	-0.42175944633560
33	0.04180810947011	-0.57501130472439
34	0.02440764897515	-0.84326542405804
35	0.01351589487357	-1.33639032314051
36	0.00712943906317	-2.27497866326982
37	0.00359475887804	-4.12355846870706
38	0.00173763283600	-7.89646555954094
39	8.072443064970693e-004	-15.88082094879666
40	3.612023608896573e-004	-33.39366890733039
41	1.559619892086842e-004	-73.16896280408443
42	6.509374294741310e-005	-1.666014960905005e+002
43	2.630049104407255e-005	-3.933152262493173e+002
44	1.030099804559497e-005	-9.609021524908767e+002
45	3.915769889672700e-006	-2.425331087723923e+003

Appendix B

B. Values of Phase Angle γ_m and Coefficient A_m

The values of phase angle γ_m (the angle between the incident and scattered waves) and coefficient A_m (which satisfies the boundary condition for the hard wall cylinder) calculated using equations (3.16) and (3.17) are provided in Tables B1 to B4, for various values of ka.

Table B.1: Values of γ_m and A_m calculated using MATLAB for $ka = 1$ and 3.

	***ka* = 1**		***ka* = 3**	
m	**γ_m (rad)**	**Absolute A_m**	**γ_m (rad)**	**Absolute A_m**
0	5.129905576941148e-001	9.815701056113450e-001	-8.070669278081472e-001	1.444523426204905e+000
1	-3.578587592841100e-001	7.005388936977347e-001	9.467491880057284e-001	1.623040535524163e+000
2	-8.323222727963338e-002	1.662723211618244e-001	-3.473541952377166e-002	6.945686989078533e-002
3	-3.554676082935588e-003	7.109337193914309e-003	-4.378482745549908e-001	8.479834067202392e-001
4	-7.586325039132730e-005	1.517265006371177e-004	-1.921537934956991e-001	3.819469792679719e-001
5	-9.677630993435400e-007	1.935526198686778e-006	-2.668523998615176e-002	5.336414599328023e-002
6	-8.185534576821557e-009	1.637106915364312e-008	-2.257226244892119e-003	4.514448656209731e-003
7	-4.926477303351291e-011	9.852954606702583e-011	-1.333990167462702e-004	2.667980327012486e-004
8	-2.218017397316136e-013	4.436034794632272e-013	-5.793427572056148e-006	1.158685514404748e-005
9	-7.752996639649086e-016	1.550599327929817e-015	-1.925552631814174e-007	3.851105263628324e-007
10	-2.165234984949363e-018	4.330469969898725e-018	-5.059024628555041e-009	1.011804925711008e-008
11	-4.942844215311344e-021	9.885688430622688e-021	-1.077866847723124e-010	2.155733695446247e-010
12	-9.396237179094143e-024	1.879247435818829e-023	-1.900886121413640e-012	3.801772242827279e-012
13	-1.510556953544256e-026	3.021113907088511e-026	-2.821849676750080e-014	5.643699353500161e-014
14	-2.080564184215395e-029	4.161128368430790e-029	-3.575871848800525e-016	7.151743697601050e-016
15	-2.482690642148102e-032	4.965381284296204e-032	-3.914292838087428e-018	7.828585676174856e-018

Table B.2: Values of γ_m and A_m calculated using MATLAB for $ka = 5$ and 10.

	***ka* = 5**		***ka* = 10**	
m	**γ_m (rad)**	**Absolute A_m**	**γ_m (rad)**	**Absolute A_m**
0	1.146794186699486e+000	1.822899435379958e+000	-1.728366890879051e-001	3.439549243654551e-001
1	-3.201103732051438e-001	6.293426577107429e-001	1.448470828374209e+000	1.985055122061599e+000
2	1.568491367272447e+000	1.999994687163952e+000	2.978193133768141e-002	5.955505790448190e-002
3	5.518774895373773e-001	1.048573825267000e+000	-1.285519169911724e+000	1.919167382153724e+000
4	-1.711381685866357e-001	3.406080017284482e-001	6.474057960114398e-001	1.206238335735818e+000
5	-4.615519094212114e-001	8.906763282257302e-001	-4.494270076194941e-001	8.688990268135356e-001
6	-2.513226110746530e-001	4.973704735767570e-001	-1.426245964905165e+000	1.979141550293708e+000
7	-5.344560443122232e-002	1.068403282069836e-001	8.718997926595900e-001	1.531105187435059e+000
8	-7.361233316724204e-003	1.472233367090385e-002	1.855528219829056e-001	3.689797883187202e-001
9	-7.592445756170732e-004	1.518489005344717e-003	-2.967895669323028e-001	5.849032902601247e-001
10	-6.082405383791230e-005	1.216481076008171e-004	-4.839316644315005e-001	9.305259277249190e-001
11	-3.888536335587284e-006	7.777072671154969e-006	-3.268596837277858e-001	6.421411266487378e-001
12	-2.031207683566750e-007	4.062415367133472e-007	-1.112006430983138e-001	2.219432159087718e-001
13	-8.840960041582735e-009	1.768192008316547e-008	-2.602393670333672e-002	5.204199874282658e-002
14	-3.258751944539170e-010	6.517503889078341e-010	-4.891519597680763e-003	9.783000182337135e-003
15	-1.031028612814559e-011	2.062057225629119e-011	-7.654584190870611e-004	1.530916688673312e-003
16			-1.012226269415207e-004	2.024452535373316e-004
17			-1.146053898817935e-005	2.292107797585693e-005
18			-1.124593778208000e-006	2.249187556415525e-006
19			-9.667628099929709e-008	1.933525619985939e-007
20			-7.348789493061785e-009	1.469757898612357e-008

Table B.3: Values of γ_m and A_m calculated using MATLAB for $ka = 15$ and 20.

	***ka* = 15**		***ka* = 20**	
m	**γ_m (rad)**	**Absolute A_m**	**γ_m (rad)**	**Absolute A_m**
0	-1.468409567169597e+000	1.989526106112857e+000	3.837755213627880e-001	7.488480212048134e-001
1	1.358731100035741e-001	2.709108509234867e-001	-1.161956013763683e+000	1.835164936100895e+000
2	-1.334306078216666e+000	1.944332535266784e+000	4.840995653939255e-001	9.308231572404798e-001
3	4.047198797823924e-001	7.875225715036970e-001	-9.610468049359370e-001	1.639582965816753e+000
4	-9.294056003052285e-001	1.602528893915081e+000	7.861227456868406e-001	1.415237905139315e+000
5	9.477214392904160e-001	1.624175988285900e+000	-5.570995325832132e-001	1.057453062333633e+000
6	-2.454061584077767e-001	4.859006684047293e-001	1.293107310234694e+000	1.923383049486138e+000
7	-1.364948539789900e+000	1.957776102201738e+000	5.437033885542456e-002	1.086871102979039e-001
8	7.336777287726852e-001	1.339211336470739e+000	-1.130702708831674e+000	1.809423567340156e+000
9	-2.286897443228369e-001	4.534031525720936e-001	8.807347599056423e-001	1.542413647842460e+000
10	-1.104898360135292e+000	1.786837073143745e+000	-1.929589279921929e-001	3.835274876059444e-001
11	1.254691622585824e+000	1.900907086523142e+000	-1.208284705726481e+000	1.870018186584987e+000
12	5.793712547193060e-001	1.094995813120668e+000	9.787276790287275e-001	1.659575974021412e+000
13	3.191313673145584e-002	6.381544005468122e-002	8.790923718903068e-002	1.755921066738230e-001
14	-3.484699701194874e-001	6.829202766725837e-001	-7.352198818432639e-001	1.341500509078510e+000
15	-4.931518759745609e-001	9.468090992651105e-001	-1.485350092813664e+000	1.992703382139249e+000
16	-3.649180648264603e-001	7.137455113727033e-001	9.866749758175952e-001	1.668393906898669e+000
17	-1.548443684402772e-001	3.084526632931428e-001	4.092206824449433e-001	7.957889573091576e-001
18	-4.667569373144138e-002	9.331749494908553e-002	-5.696155097379290e-002	1.138615057778784e-001
19	-1.159765272778880e-002	2.319478547619298e-002	-3.779295513914702e-001	7.379938467228678e-001
20	-2.478440636635322e-003	4.956876198526215e-003	-4.983845887514055e-001	9.560145138711387e-001
21	-4.614014243027709e-004	9.228028158627629e-004	-3.885374559080056e-001	7.576705774123097e-001
22	-7.548880577554636e-005	1.509776114077002e-004	-1.885313290668023e-001	3.748329014696935e-001
23	-1.094636728777335e-005	2.189273457510948e-005	-6.658664646475423e-002	1.330749045302063e-001
24	-1.418079638116890e-006	2.836159276232830e-006	-1.963861688027927e-002	3.927470909960197e-002
25	-1.653043508449735e-007	3.306087016899455e-007	-5.073392324601202e-003	1.014674112071970e-002
26	-1.744887942892248e-008	3.489775885784497e-008	-1.163705092404372e-003	2.327409659508599e-003
27	-1.677147095982643e-009	3.354294191965287e-009	-2.386425913610900e-004	4.772851781919254e-004
28	-1.475156117706648e-010	2.950312235413296e-010	-4.403067945144659e-005	8.806135887443909e-005
29	-1.192550538887372e-011	2.385101077774745e-011	-7.354542781579203e-006	1.470908556302580e-005
30	-8.896084926199342e-013	1.779216985239868e-012	-1.118573351024911e-006	2.237146702049354e-006
31			-1.557246207634564e-007	3.114492415269115e-007
32			-1.993733701668540e-008	3.987467403337080e-008
33			-2.357264425422621e-009	4.714528850845241e-009
34			-2.583481679882387e-010	5.166963359764773e-010
35			-2.633423480662658e-011	5.266846961325315e-011

Table B.4: Values of γ_m and A_m calculated using MATLAB for $ka = 25$ and 30.

	***ka* = 25**		***ka* = 30**	
m	**γ_m (rad)**	**Absolute A_m**	**γ_m (rad)**	**Absolute A_m**
0	-9.031498545162312e-001	1.570562002874435e+000	9.527618930620101e-001	1.630037893699097e+000
1	6.876797027321421e-001	1.269491900638269e+000	-6.013485183944878e-001	1.131509879828849e+000
2	-8.229841507836738e-001	1.466356844348570e+000	1.019524387811775e+000	1.703718012714104e+000
3	8.481427419518632e-001	1.500106702199820e+000	-4.677479980047470e-001	9.017546502068058e-001
4	-5.819584734936241e-001	1.099322149335750e+000	1.220114790829969e+000	1.878277595024381e+000
5	1.170134202011234e+000	1.841605897170514e+000	-1.999379145395230e-001	3.972169650548421e-001
6	-1.784537452343424e-001	3.550161740243803e-001	1.555454777805881e+000	1.999764641490898e+000
7	-1.485739486799945e+000	1.992769694617742e+000	2.033260575782419e-001	4.038559674973831e-001
8	3.903461629514864e-001	7.610171231760509e-001	-1.114467482533474e+000	1.795352516579824e+000
9	-8.328101446455971e-001	1.479649906859031e+000	7.439793764119969e-001	1.354442418842547e+000
10	1.128656011584647e+000	1.807675893780715e+000	-5.041535231015206e-001	9.661329042161707e-001
11	-7.639202562924609e-003	1.527825652490938e-002	1.424741752443500e+000	1.978705955324396e+000
12	-1.099159431544762e+000	1.781651533343220e+000	2.479660405334953e-001	4.908654405343420e-001
13	9.968002299998394e-001	1.679475673880457e+000	-8.923308602923813e-001	1.557073413638677e+000
14	-1.629204890077758e-003	3.258408338684871e-003	1.146081170131993e+000	1.822312285641953e+000
15	-9.512856066505748e-001	1.628325296063118e+000	8.074632993221909e-002	1.613172291868681e-001
16	1.291316189698432e+000	1.922397950975966e+000	-9.459062793819344e-001	1.622054895123637e+000
17	4.453095560580564e-001	8.614745365433665e-001	1.208678627626263e+000	1.870297429601288e+000
18	-3.448090866225010e-001	6.760340143849237e-001	2.624298564125032e-001	5.188559590788061e-001
19	-1.075293277870644e+000	1.759459268686940e+000	-6.417603508745922e-001	1.197212970594315e+000
20	1.400481140085656e+000	1.971062787854546e+000	-1.502360033580368e+000	1.995318301437199e+000
21	8.064537024673810e-001	1.443674917017773e+000	8.240545286761650e-001	1.467811795755167e+000
22	2.950015364445492e-001	5.814826403934716e-001	5.652670170012471e-002	1.129932070311056e-001
23	-1.163014110812219e-001	2.320788116750408e-001	-6.605728747200401e-001	1.227138635838244e+000
24	-3.973808551863186e-001	7.740092345055428e-001	-1.323671608228672e+000	1.939239543253116e+000
25	-5.018244485089077e-001	9.620516880035583e-001	1.213608860155135e+000	1.873767807548617e+000
26	-4.048917115995046e-001	7.878384598645760e-001	6.748369388880091e-001	1.249540010953998e+000
27	-2.153640823416572e-001	4.274062280120701e-001	2.117563044458241e-001	4.203545949970555e-001
28	-8.507548532012769e-002	1.699457907080428e-001	-1.593402323536887e-001	3.173336627305930e-001
29	-2.828773423760244e-002	5.656792353401878e-002	-4.113642803623179e-001	7.997203331336086e-001
30	-8.332758389048688e-003	1.666532391745631e-002	-5.042879110602239e-001	9.663682313014828e-001
31	-2.207806324585138e-003	4.415609061920983e-003	-4.170130360408832e-001	8.100625487007372e-001
32	-5.294548043237669e-004	1.058909559174856e-003	-2.373158963960077e-001	4.701892030906603e-001
33	-1.154955589765259e-004	2.309911174395115e-004	-1.020450977085217e-001	2.037361743879085e-001
34	-2.303192751755968e-005	4.606385503104678e-005	-3.714208388743552e-002	7.426708935884561e-002
35	-4.219049314865390e-006	8.438098629705748e-006	-1.206761990000982e-002	2.413465401204692e-002
36	-7.131117045746308e-007	1.426223409149141e-006	-3.559560663551193e-003	7.119106293340530e-003
37	-1.116653043475810e-007	2.233306086951615e-007	-9.591420692166756e-004	1.918283844311328e-003
38	-1.625849470486460e-008	3.251698940972920e-008	-2.370887376238219e-004	4.741774708053066e-004
39	-2.208358866419114e-009	4.416717732838228e-009	-5.398358616045319e-005	1.079671722684662e-004
40	-2.806559057706346e-010	5.613118115412692e-010	-1.136853624796371e-005	2.273707249543764e-005
41			-2.222907048356745e-006	4.445814096709828e-006
42			-4.050070638628128e-007	8.100141277256036e-007
43			-6.898237394153560e-008	1.379647478830711e-007
44			-1.101601694100731e-008	2.203203388201461e-008
45			-1.653786687641506e-009	3.307573375283011e-009

Appendix C

C. *Wronskian* Relationship

The left hand side of equation (3.25), in Chapter 3, is

$$J_m(ka)\,H'_m(ka) - J'_m(ka)\,H_m(ka). \tag{C.1}$$

Using equation (3.12), and solving the above equation (C.1) gives

$$\begin{aligned} & J_m(ka)\left[J'_m(ka) + i\,N'_m(ka)\right] - J'_m(ka)\left[J_m(ka) + i\,N_m(ka)\right] \\ &= J_m(ka)\,J'_m(ka) + i\,J_m(ka)\,N'_m(ka) - J_m(ka)\,J'_m(ka) - i\,J'_m(ka)\,N_m(ka) \\ &= i\,J_m(ka)\,N'_m(ka) - i\,J'_m(ka)\,N_m(ka) \\ &= i\left[J_m(ka)\,N'_m(ka) - J'_m(ka)\,N_m(ka)\right]. \end{aligned} \tag{C.2}$$

According to *Wronskian* (Junger & Feit, 1993)

$$J_m(ka)\,N'_m(ka) - J'_m(ka)\,N_m(ka) = \frac{2}{\pi ka}. \tag{C.3}$$

Now, substituting equation (C.3) in equation ((C.2), one can find out the *Wronskian* relationship for equation (C.1), which is

$$J_m(ka)\,H'_m(ka) - J'_m(ka)\,H_m(ka) = \frac{2i}{\pi ka}. \tag{C.4}$$

Appendix D

D. Corrections in the Real-time theory presented by Friot *et al.*, (2004):

The mathematical derivations given by Friot *et al*., (2004) are same to those by Junger & Feit (1993); the later derivations have already been discussed and presented in Section 3.4 in Chapter 3, of this thesis. First of all, the equations for sound pressure field of a cylinder are given by (Friot *et al*., 2004)

$$p_s(\rho,\phi) = -i\,\omega\rho_v \sum_{n=0}^{\infty} \varepsilon_n (-i)^n \frac{J'_n(ka)}{H'^{(1)}_n(ka)} H^{(1)}_n(k\rho)\cos(n\varphi); \qquad \text{(D.1)}$$

$$p_s(\rho,\phi) = i\,\omega\rho_i \sum_{n=0}^{\infty} \varepsilon_n \left[J_n(k\rho_{\inf}) - \frac{J'_n(ka)}{H'^{(1)}_n(ka)} H^{(1)}_n(k\rho_{\inf}) \right] H^{(1)}_n(k\rho_{\sup})\cos(n\varphi), \qquad \text{(D.2)}$$

where equation (D.1) is for scattered sound pressure and ρ_v is the fluid density. The Authors have mentioned in their work that equation (D.2) is also for scattered sound pressure and denoted it by p_s, same as denoted the scattered sound pressure in equation (D.1). Apparently, equation (D.2) is for total sound pressure, because it is addition of incident and scattered sound pressures, as already shown in equation (3.21) in Chapter 3. It is noticeable in equation (D.2); $H^{(1)}_n(k\rho_{\inf})$ term has been used for the scattered waves. According to the Authors, $H^{(1)}_n$ represents the *Hankel function* for the outgoing waves. However, they have used a supplement term $H^{(1)}_n(k\rho_{\sup})$ in equation (D.2), for an infinite line of monopoles parallel to the cylinder at some coordinates, which is ambiguous and not making it clear whether that represents the incoming waves or outgoing waves.

Appendix E

E. Rocket Engine Noise Prediction Comparison with *Gierke Method*

According to *Gierke Method*, the overall acoustic power level of a rocket engine can be determined by the following expression (Potter & Crocker, 1966)

$$L_w = 78 + 13.5 \log_{10} (0.676\, U_e\, F) \qquad \text{(E.1)}$$

where

U_e = exhaust velocity, m/s

F = thrust of the engine, N

Using the specifications given for engine 'E' in Table 9.1 in Chapter 9, and solving the above equation (E.1), the overall acoustic power level of engine 'E' is

$$L_w = 78 + 13.5 \log_{10} \left[(0.676)(2670)(31803)\right]$$

$$L_w = 182.75 \text{ dB}$$

Recalling equation (9.2), the overall acoustic power level of engine 'E' is

$$L_w = 120 + 10 \log_{10} \left[(0.005)(31803)(2670)\right]$$

$$L_w = 176.28 \text{ dB}$$

The difference between the results obtained using equation (E.1) and (9.2) is 6.47dB.

References

Abramowitz, M. and Stegun, I. A. (1965) *Handbook of Mathematical Functions*, National Bureau of Standards, Applied Math, Series No. 55, Dover Publications.

Agrest, M. M. and Maksimov, M. S. (1971) *Theory of Iincomplete Cylindrical Functions and their Applications*, Springer-Verlag, Berlin.

Bies, D. A. and Hansen, C. H. (2003) *Engineering Noise Control*, Spon Press, London, 3rd Edition.

Chemoul, B. (1999) "Control of the Ariane 5 Vibrations: the Development Program Challenges", *Proceeding of Launch Vehicle Vibrations*, First European Conference on Launcher Technology, France, 14-16 Dec, 1999, Centre National D'Etudes Spatiales, p31-52.

Ciskowski, R. D. and Brebbia, C. A. (1991) *Boundary Element Methods in Acoustics*, Computational Mechanics Publications, Southampton.

Cole, J. N., Von Gierke, H. E., Kyrasis, D. T., Eldred, K. Mck. and Humphrey, A. J. (1957) "Noise Radiation from Fourteen Types of Rockets in the 1,000 to 130,000 Pound Thrust Range", WADC TR 57-354.

Cunefare, K. A. and Koopmann G. (1989) "A Boundary Element Method for Acoustic Radiation Valid for all Wavenumbers", *Journal of the Acoustical Society of America*, **85**(1), 39-48.

Cutanda, V. (1999) "Numerical Transducer Modelling", *Proceeding of the 6th*

International Congress on Sound and Vibration 1999, 560-570.

Dementjev, V. C., Koudriavtsev, V. V., Rybak, S. P., Safronov, A. V. and Troclet, B. (1999) "Technique for Predicting the Acoustical Environment Resulting from a Launch Vehicle Engine Jets Interaction with Launch Pad", *Proceeding of Launch Vehicle Vibrations*, First European Conference on Launcher Technology, France, 14-16 Dec, 1999, Centre National D'Etudes Spatiales, p169-178.

Dumnov, G., Mel'nikov, D. and Komarov, V. (2000) "Acoustics Loads on Rockets During Launching", *American Institute of Aeronautics and Astronautics (AIAA)*, 2000-3742.

Eldred, K. M., Roberts, W. and White, R. (1961) "Structural Vibrations in Space Vehicles", WADD TR 61-62.

Eldred, K. M., White, R., Mann, M. and Cottis, M. (1963) "Suppression of Jet Noise with Emphasis on the Near Field", ASD-TDR-62-578, Wright Paterson AFB, Ohio, USA.

Elias, G. (2000) "Ariane 5 at Lift Off: Localization and Ranking of Acoustic Sources", in *Inter Noise 2000*, *29th International Congress and Exhibition on Noise and Control Engineering*, 27-30 August 2000, Nice, France.

Epstein, R. J. and Bliss, D. B. (1997) "A Boundary Element Method Using Analytical/Numerical Matching", *Journal of the Acoustical Society of America*, **101**(1), 92-106.

Estève, S. J. and Johnson, M. E. (2002a) "Reduction of Sound Transmission into a Circular Cylindrical Shell Using Distributed Vibration Absorbers and Helmholtz Resonators",

Journal of the Acoustical Society of America, **112**(6), 2840-2848.

Estève, S. J. and Johnson, M. E. (2002b) "Control of the Noise Transmitted into a Cylinder Using Optimally Damped Helmholtz Resonators and Distributed Vibration Absorbers" Presented at ICSV9, 2002.

Fahnline, J. B. and Koopmann, G. H. (1991) "A Numerical Solution for the General Radiation Problem Based on the Combined Methods of Superposition and Singular-Value Decomposition", *Journal of the Acoustical Society of America*, **90**(5), 2808-2819.

Fahy, F. (1987) *Sound and Structural Vibration*, Academic Press Inc. Ltd., London.

Fahy, F. and Walker, J. (1998) *Fundamentals of Noise and Vibration*, E & FN Spon, London.

Filippi, P., Habault, D. Lefebvre, JP. and Bergassoli, A. (1999) *Acoustics*: *Basic Physics, Theory and Methods*, Academic press, Harcourt Brace & Company.

Francis, D. T. I (1993) "A Gradient Formulation of the Helmholtz Integral Equation for Acoustic Radiation and Scattering", *Journal of the Acoustical Society of America*, **93**(4), 1700-1709.

Franken, P. A., Kerwin, E. M. and Staff of Bolt Beranek and Newman Inc. (1960) "Methods of Space Vehicle Noise Prediction", WADC TR 58-343, Wright Paterson AFB, Ohio, USA.

Friot, E. and Bordier, C. (2004) "Real-Time Active Suppression of Scattered Acoustic Radiation", *Journal of Sound and Vibration*, **278**, 563-580.

Fuller, C. R. (1989) "Free-field Correction Factor for Spherical Acoustic Waves Impinging on Cylinders", *American Institute of Aeronautics and Astronautics (AIAA)*, **27(12)**, 1722 - 1726.

Fuller, C. R. (1986) "Analytical Model for Investigation of Interior Noise in Aircraft with Multiple Propellers Including Synchrophasing", *Journal of Sound and Vibration*, **109(1)**, 141 - 156.

Gardonio, P., Ferguson, N. S. and Fahy, F. J. (2001) "A Modal Expansion Analysis of Noise Transmission Through Circular Cylindrical Shell Structures with Blocking Masses", *Journal of Sound and Vibration*, **244**(2), 259-297.

Gély, D., Elias, G. and Bresson, C. (2000) "Reduction of Supersonic Jet Noise. Application to the Ariane 5 Launch Vehicle", *American Institute of Aeronautics and Astronautics (AIAA)*, 2000-2026.

Hansen, C. H., Zander, A. C. and Howard, C. Q. (2000a) "Investigation of Passive Control Devices for Potential Application to a Launch Vehicle Structure to Reduce the Interior Noise Levels During Launch: Progress Report for Stage One", Technical Report, Department of Mechanical Engineering, University of Adelaide, S. A. 5005, Australia.

Hansen, C. H., Zander, A. C., Cazzolato, B. S. and Morgans, R. C. (2000b) "Investigation of Passive Control Devices for Potential Application to a Launch Vehicle Structure to Reduce the Interior Noise Levels During Launch: Final Report for Stage One", Technical Report, Department of Mechanical Engineering, University of Adelaide, S. A. 5005, Australia.

Hansen, C.H., Zander, A.C., Cazzolato, B.S. and Morgans, R.C. (2001a) "Investigation of

Passive Control Devices for Potential Application to a Launch Vehicle Structure to Reduce the Interior Noise Levels During Launch: Preliminary Report for Stage Two", Technical Report, Department of Mechanical Engineering, University of Adelaide, S. A. 5005, Australia.

Hansen, C.H., Zander, A.C., Cazzolato, B.S. and Morgans, R.C. (2001b) "Investigation of Passive Control Devices for Potential Application to a Launch Vehicle Structure to Reduce the Interior Noise Levels During Launch: Final Report for Stage Two", Technical Report, Department of Mechanical Engineering, University of Adelaide, S. A. 5005, Australia.

Howard, C. Q., Hansen, C. H., Morgans, R. C. and Zander, A. C. (2003a) "Investigation of Passive Control Devices for Potential Application to a Launch Vehicle Structure to Reduce the Interior Noise Levels During Launch: Final Report for Stage 3A", Technical Report, Department of Mechanical Engineering, University of Adelaide, S. A. 5005, Australia.

Howard, C. Q., Hansen, C. H., Morgans, R. C. and Zander, A. C. (2003b) "Investigation of Passive Control Devices for Potential Application to a Launch Vehicle Structure to Reduce the Interior Noise Levels During Launch: Final Report for Stage 3B", Technical Report, Department of Mechanical Engineering, University of Adelaide, S. A. 5005, Australia.

Howard, C. Q., Hansen, C. H., Morgans, R. C. and Zander, A. C. (2004) "Investigation of Passive Control Devices for Potential Application to a Launch Vehicle Structure to Reduce the Interior Noise Levels During Launch: Report for Stage 4, Tasks 1 and 2", Technical Report, Department of Mechanical Engineering, University of Adelaide, S. A. 5005, Australia.

Hwang, J and Chang, S. (1991) "A Retracted Boundary Integral Equation for Exterior

Acoustic Problem with Unique Solution for all Wave Numbers", *Journal of the Acoustical Society of America*, **90**(2), 1167-1180.

Jeans, A. and Mathews, I. C. (1992) "The Wave Superposition Method as a Robust Technique for Computing Acoustic Fields", *Journal of the Acoustical Society of America*, **92**(2), 1156-1166.

Johnson, M. E., Fuller, C. R. and Marcotte, P. (2001) "Optimization of Distributed Vibration Absorber for Sound Transmission into a Composite Cylinder", *Proceedings of the 7th AIAA/CEAS Aeroacoustics Conference*, May 2001, Paper AIAA-2001-2232.

Juhl, P. M. (1993) "The Boundary Element Method for Sound Field Calculations", The Acoustic Laboratory, Technical University of Denmark.

Junger, C. M. and Feit, D. (1993) *Sound Structure and Their Interaction*, Acoustical Society of America, Chapter 10.

Kinsler, L. E., Coppens, A. B., Frey, A. R. and Sanders, J. V. (1982) *Fundamentals of Acoustics*, Jhon Wiley & Sons, Inc., 3rd edition.

Kleinman, R. E., Roach, G. F., Schuetz, L. S. and Shirron, J. (1988) "An Iterative Solution to Acoustic Scattering by Rigid Objects", *Journal of the Acoustical Society of America*, **84**(1), 385-391.

Koopmann, G. H., Song, L. and Fahnline, J. B. (1989) "A Method for Computing Acoustic Fields Based on the Principle of Wave Superposition", *Journal of the Acoustical Society of*

America, **86**(6), 2433-2438.

Kreyszig, E. (1983) *Advanced Engineering Mathematics*, 5th Edition, John Wiley & Sons, Inc.

Lassiter, L. W. and Heitkotter, R. H. (1954) "Some Measurements of Noise from Three Solid-Fuel Rocket Engines", NASA TN-3316.

Malbequi, P., Candel, S. M. and Rignot, E. (1987) "Boundary Integral Calculations of Scattered Field: Application to a Spacecraft Launcher", *Journal of the Acoustical Society of America*, **82**(5), 1771-1781.

Margasahayam, R. and Caimi, R. (1999) "Rocket Noise Prediction Program", *Sixth International Congress on Sound and Vibration,* 5-8 July, 1999, Copenhagen, Denmark (also available as NASA Tech. Briefs, KSC-12061, Florida, USA).

Martinez, R. (1991) "The Thin-Shape Breakdown (TSB) of the Helmholtz Integral Equation", *Journal of the Acoustical Society of America*, **90**(5), 2728-2738.

Mayes, W. H., Lanford, W. E. and Hubbard, H. H. (1959) "Near Field and Far Field Noise Surveys of Solid Fuel Rocket Engines for a Range of Nozzle Exit Pressures", NASA TN D-21.

McLachlan, N. W. (1941) *Bessel Functions for Engineers*, Oxford University Press, London.

Mel'nikov, D. A., Komarov, V. V., Dumnov, G. E. and Dement'ev, V. K. (1999) "An Experimental Investigation of the Acoustic Field Appearing During Rocket Ascent from a

Launching pad", *Proceeding of Launch Vehicle Vibrations*, First European Conference on Launcher Technology, France, 14-16 Dec, 1999, Centre National D'Etudes Spatiales, p147-155.

Morgan, W. V., Sutherland, L. C. and Young, K. J. (1961) "The Use of Acoustic Scale Models for Investigating Near Field Noise of Jet and Rocket Engines", WADD TR 61-178, Wright Paterson AFB, Ohio, USA.

Morgans, R. C., Zander, A. C., Hansen, C. H. and Murphy, D. J. (2004) "Fast Boundary Element Models for Far Field Pressure Prediction", *Proceedings of acoustics 2004*.

Morse, P. M. (1936) *Vibration and Sound*, McGraw-Hill Inc.

Morse, P. M. and Feshbach, H. (1953a) *Methods of Theoretical Physics Part-I*, McGraw-Hill Inc.

Morse, P. M. and Feshbach, H. (1953b) *Methods of Theoretical Physics Part-II*, McGraw-Hill Inc.

Morse, P. M. and Ingard, K. U. (1986) *Theoretical Acoustics*, McGraw-Hill Inc.

NASA-SP-8072 (1971) "Acoustic Loads Generated by the Propulsion System", Space Vehicle Design Criteria (Structures).

NASA PN PD-ED-1259 (1996) "Acoustic Noise Requirement", Preferred Reliability Practices, http://techinfo.jpl.nasa.gov/practice/1259.pdf.

Nye, J. F. (2003) "Spurious Internal Fields in Scattering by a Cylinder", *Journal of*

Physics- A: Mathematical and General, **36**, 4221-4237.

O'Neil, P. V. (1995) *Advanced Engineering Mathematics*, PWS Publishing Company, 4th edition.

Pierce, A. D. (1981) *Acoustics*: *an Introduction to Physical Principles and Applications*, McGraw-Hill Book Company.

Potter, R. C. (1966) "Correlation Patterns of the Acoustic Pressure Fluctuations on the S-IC Vehicle Due to the Exhaust Noise of the Test and Launch Stand", Report WR 66-15, Contract NAS8-20073-1, Wyle Labs.

Potter, R. C. and Crocker, M. J. (1966) "Acoustic Prediction Methods for Rocket Engines, Including the Effects of Clustered Engines and Deflected Exhaust Flow", NASA CR-566.

Rogerio, P., Wim, D., Bert, P., Paul, S. and Luis, C. S. G. (2002) "Vibro-Acoustic Analysis of the Brazilian Vehicle Satellite Launcher (VLS) Fairing", *Proceedings of ISMA 2002*, Volume V, 2075-2083.

Seybert, A. F., Soenarko, B., Rizzo, F. J. and Shippy, D. J. (1985) "An Advanced Computational Method for Radiation and Scattering of Acoustic Waves in Three Dimensions", *Journal of the Acoustical Society of America*, **77**(2), 362-368.

Seybert, A. F., Soenarko, B., Rizzo, F. J. and Shippy, D. J. (1986) "A Special Integral Equation Formulation for Acoustic Radiation and Scattering for Axisymmetric Bodies and Boundary Conditions", *Journal of the Acoustical Society of America*, **80**(4), 1241-1247.

Seybert, A. F. and Rengarajan, T. K. (1987) "The Use of CHIEF to Obtain Unique Solutions for Acoustic Radiation Using Boundary Integral Equations", *Journal of the Acoustical Society of America*, **81**(5), 1299-1306.

Seybert, A.F., and Casey, D. K. (1988) "An Integral Equation Method for Coupled Fluid/Fluid Scattering in Three Dimensions", *Journal of the Acoustical Society of America*, **84**(1), 379-384.

Seybert, A. F., Cheng, C. Y. R. and Wu, T. W. (1990) "The Solution of Coupled Interior / Exterior Acoustic Problems Using the Boundary Element Method", *Journal of the Acoustical Society of America*, **88**(3), 1612-1618.

Song, L., Koopmann, G. H. and Fahnline, J. B. (1991a) "Active Control of the Acoustic Radiation of a Vibrating Structure Using a Superposition Formulation", *Journal of the Acoustical Society of America*, **89**(6), 2786-2792.

Song, L., Koopmann, G. H. and Fahnline, J. B. (1991b) "Numerical Errors Associated with the Method of Superposition for Computing Acoustic Fields", *Journal of Acoustical Society of America*, **89**(6), 2625-2633.

Tedrick, R. N. (1964) "Acoustical Measurements of Static Tests of Clustered and Single-Nozzled Rocket Engines", *Journal of the Acoustical Society of America*, **36**(11), 2027-2032.

Troclet, B., Chemoul, B., Roux, P., Gely, D. and Elias, G. (1999) "Synthesis of Vibroacoustic Studies Performed During Ariane 5 Program", *Proceeding of Launch Vehicle Vibrations*, First European Conference on Launcher Technology, France, 14-16

Dec, 1999, Centre National D'Etudes Spatiales, p201-210.

Wu, T. W. (2000) *Boundary Element Acoustics*: *Fundamentals and Computer Codes*, WIT Press, USA.